Title
Benefits of Two Mitigation Strategies for Container Vessels: Cleaner Engines and Cleaner Fuels

Journal
Environmental Science & Technology, 46(9)

ISSN
0013-936X 1520-5851

Authors
Khan, M. Yusuf
Giordano, Michael
Gutierrez, James
et al.

Publication Date
2012-04-11

DOI
10.1021/es2043646

Peer reviewed

Environmental Science & Technology

Article

pubs.acs.org/est

Benefits of Two Mitigation Strategies for Container Vessels: Cleaner Engines and Cleaner Fuels

M. Yusuf Khan,[†,‡] Michael Giordano,[†,‡] James Gutierrez,[†,‡] William A. Welch,[‡] A. Asa-Awuku,[†,‡] J. Wayne Miller,[†,‡] and David R. Cocker, III*[,†,‡]

[†]Department of Chemical and Environmental Engineering, Bourns College of Engineering, University of California, Riverside, California 92521, United States

[‡]College of Engineering—Center for Environmental Research and Technology, University of California, Riverside, 1084 Columbia Avenue, Riverside, California 92507, United States

Supporting Information

ABSTRACT: Emissions from ocean-going vessels (OGVs) are a signifi cant health concern for people near port communities. This paper reports the emission benefits for two mitigation strategies, cleaner engines and cleaner fuels, for a 2010 container vessel. In-use emissions were measured following International Organization for Standardization (ISO) protocols. The overall in-use nitrogen oxide (NO_x) emission factor was 16.1 ± 0.1 gkW^{-1} h^{-1}, lower than the Tier 1 certification (17 gkW^{-1} h^{-1}) and significantly lower than the benchmark value of 18.7 gkW^{-1} h^{-1} commonly used for estimating emission inventories. The in-use particulate matter ($PM_{2.5}$) emission was 1.42 ± 0.04 gkW^{-1} h^{-1} for heavy fuel oil (HFO) containing 2.51 wt % sulfur. Unimodal (~30 nm) and bimodal (~35 nm; ~75 nm) particle number size distributions (NSDs) were observed when the vessel operated on marine gas oil (MGO) and HFO, respectively. First-time emission measurements during fuel switching (required 24 nautical miles from coastline) showed that concentrations of sulfur dioxide (SO_2) and particle NSD took ~55 min to reach steady-state when switching from MGO to HFO and ~84 min in the opposite direction. Therefore, if OGVs commence fuel change at the regulated boundary, then vessels can travel up to 90% of the distance to the port before steady-state values are re-established. The transient behavior follows a classic, nonlinear mixing function driven by the amount of fuel in day tank and the fuel consumption rate. Hence, to achieve the maximum benefits from a fuel change regulation, fuel switch boundary should be further increased to provide the intended benefits for the people living near the ports.

INTRODUCTION

Globalization and continuous growth in international trade has led to larger and more powerful engines on ocean-going vessels (OGVs). The diesel engines on the OGVs are relatively high emitters of $PM_{2.5}$, NO_x, sulfur oxides (SO_x), and carbon dioxide (CO_2), a consequence of the combination of using heavy fuel oil and few emission regulations. Increasing ship emissions affect global climate[1−3] and regional air quality near port communities,[4,5] suggesting that mitigation strategies and controls are needed to reduce the impact of OGV emissions and shipping-related PM mortalities.[6] Two mitigation strategies were investigated in this research: use of a cleaner burning modern diesel engine and the switch to cleaner, lower-sulfur fuels near coastal communities.

The current emission standards do not include limits on PM mass emissions; however, it is well established that reducing fuel sulfur content is effective in lowering SO_x and PM mass emissions from combustion sources. The approach is based on the fact that SO_2 is formed during the fast reaction of fuel-sulfur with oxygen in the combustion process, and subsequently, particles form during the slower oxidation of sulfur dioxide and its hydration to sulfuric acid (eq 1).

$$S + O_2 \xrightarrow{(Fast)} SO_2 \xrightarrow{1/2O_2(Slow)} SO_3 \xrightarrow{(H_2O)} \text{Sulfuric acid} \quad (1)$$

Research shows that the sulfur content for heavy fuel oil is the primary factor contributing to PM mass emissions.[28,29]

Recent shipping regulations have tightened the emission limits for NO_x and SO_x and fuel quality in global and designated emission control areas (ECAs). The International Maritime Organization (IMO) set progressive reductions in NO_x emissions and fuel sulfur content. From 2010 to 2015, fuel used by all vessels operating in ECAs cannot exceed 10 000 ppm sulfur. After 2015, fuel used in ECAs may not exceed 1000 ppm sulfur. In contrast, the sulfur content of fuel used in on-road vehicles is <15 ppm. The reduction in PM mass emissions is expected to reduce annual premature ship-related

Received: December 6, 2011
Revised: March 25, 2012
Accepted: April 2, 2012
Published: April 2, 2012

mortality by 50% in ECAs.[7] In addition to the fuel change, the California Air Resources Board (CARB) currently requires that OGV main and auxiliary engines burn fuel with sulfur content equal to or less than 1.5 wt % within 24 nautical miles (nmi) of the California coastline.[8]

Particle emissions have been previously characterized from slow-speed marine engines using test rigs, stack and plume studies during ship transit. Kasper et al.[9] reported a mean diameter of particles of 20−40 nm for a two-stroke marine diesel engine operating on a test rig and burning a heavy fuel oil (HFO) with 0.6 wt % sulfur. Petzold et al.[10] reported physical properties, chemical composition, and cloud-forming potential of particulate emissions from a 4-stroke, medium-speed, marine diesel engine operating on a test rig for load conditions from 10% to 110% with HFO containing 2.21 wt % sulfur. Moldanová[11] reported microphysical and chemical properties of the exhaust for various load conditions of a 2-stroke diesel engine and observed bimodal particle mass size distribution with peaks at 0.5 and 7 μm. Fridell et al.[12] used a cascade impactor to study the size distribution of particles from the exhaust of three transiting ships. Lyyranen et al.[13,14] studied particle number size distributions (NSDs) from 4-stroke medium speed engines operating on HFO with 2.4 wt % sulfur. Murphy et al.[15] measured criteria emissions, cloud condensation nuclei (CCN) concentrations, and estimated the particle number emission factors from simultaneous on-board (3.01 wt % sulfur) and aircraft measurements.

The contribution of ship emissions to local inventories require knowledge of emission factors (EFs) with most researchers using either data compiled by IVL Swedish Environmental Research Institute (IVL) for ENTEC UK[26] or Lloyd's register (LR).[31] In each study, only 3 container vessels were tested to represent thousands of container vessels that sail around the globe. A similar number of measurements were made from variety of vessels (tankers, ferries, tugboat, etc.). In total, the IVL EFs, which are widely used, are based on eight measurements from slow speed diesel (SSD) engines and LR EFs are from 11 SSD engines. For practical inventory development, these EFs are applied to SSD engines irrespective of vessel type; they only depend on the type of engine, fuel, and operating mode. Hence the EFs from this study are especially important as they represent the first in-use measurements from a modern container vessel using the latest Tier 1 engine technology.

Under the current certification scheme, engines are allowed to be certified while operating on distillate fuel (nitrogen free) both on test-bed and in-use even though the OGVs operate on HFO in international boundaries. The fuel-bound nitrogen can account for up to 10% of NO_x emissions which can effectively bias the certified NO_x emission to a lower value. In this study, data were collected at sea near the prescribed OGV certification load points and during fuel switching between marine gas oil (MGO) and HFO fuel. This research provides the first comparison of Tier 1 certification values with in-use data obtained from a modern container vessel (launched in 2010) at sea. Additional information is provided on the transition in emissions, particle size, and particle number during fuel switch. A nonlinear equation representing the fuel mixing process is verified as an approach to estimate the time required to switch fuels.

EXPERIMENTAL METHODS

Vessel and Engine Description. A 2010 post-Panamax container vessel was tested (Table S1) as it is representative of the large container vessels and slow-speed diesel engines being built today. The main propulsion engine (Hyundai B&W 11K98ME7) for the vessel was an electronically controlled, slow speed two-stroke, 68 530 kW diesel engine rated at 97 rpm with a displacement of 22 060 L (Table S2). The engine was equipped with the latest technology to meet IMO Tier 1 emission specifications for vessel construction between 2000 and 2010. The engine was designed with low-NO_x slide valves, an electronic fuel injection system, and improvements in the in-cylinder combustion for lowering NO_x emissions and improving fuel economy.

Fuel Properties. Emissions were evaluated for two fuel types: MGO and HFO. In compliance with California regulations, MGO with 0.17 wt % sulfur was used in the main engine within 24 nmi of the California coastline. Outside 24 nmi, the engine operated on HFO with 2.51 wt % sulfur. One-liter fuel samples were drawn from the main engine final filter drains, immediately upstream of the injector rail, for analysis of fuel properties (Table 1).

Table 1. Selected Fuel Properties

		certificate of analysis (CoA)		collected samples	
fuel	units	HFO	MGO	HFO	MGO
density @15C	kg/m^3	988.8	845.5	-	-
viscosity @40C	mm^2/s	368.6	3.3	-	-
sulfur	% m/m	2.40	0.17	2.51	0.17
ash	% m/m	0.07	<0.01	-	-
vanadium	mg/kg	262	<1	-	-
density @15.5C	kg/m^3	-	-	988.2	845.2

Test Cycles. HFO emissions at 90%, 75%, 47%, and 24% of full load were evaluated. Efforts were made to achieve loads similar to those specified in the ISO 8178-E3 test cycle (Table 2) to compare measured in-use emissions with the engine certification values; however, the actual loads at sea only approximate those in the E3 test cycle due to perturbations in loads caused by the interactions of the vessel and sea. Data for the engine load (kW), engine speed (rpm), and fuel consumption (kg/h) were downloaded from the engine computer. A check of the accuracy of the gauge readings was carried out by calculating the engine efficiency using the reported engine load and fuel consumption. At 90% and 75% engine load, efficiencies were 46.9% and 47.5% which is slow-speed diesel engines.[35] Specific fuel oil consumption (SFOC) is calculated based on fuel consumption and engine load. Measurements were also made at slower speeds, 12% and 23% of full load, while the engine operated on MGO. Additional real-time emission measurements were conducted while the engine followed typical operating conditions (including fuel switching).

Sampling and Analysis. Sampling and analysis of gases and PM conformed to ISO 8178-2 requirements.[16] Briefly, testing was conducted using a partial flow dilution system with a single venturi.[17,18] The dilution tunnel was attached directly to the stack negating the need for a heated transfer line. Dilution ratios (DRs) were obtained from both CO_2 and NO_x measurements of raw and dilute exhaust gas with DRs agreeing within 5% for the two gases. Carbon monoxide (CO), CO_2, NO_x, and SO_2 were monitored using the Horiba PG-250 Exhaust Gas Analyzer. SO_2 EFs were calculated from the fuel sulfur content per ISO 8178-1 protocol[19] except during the fuel switch when a Horiba Analyzer was used to monitor the continuous change in SO_2 exhaust concentration.

$PM_{2.5}$ samples were taken from the dilution tunnel after a 2.5-μm cyclone separator, collected on filter media, and the mass was determined gravimetrically on preweighed 47-mm-diameter

Table 2. Engine Operating Conditions

targeted modes	ISO100	ISO75	ISO50	ISO25	MGO23	MGO12	fuel switch	
fuel	HFO	HFO	HFO	HFO	MGO	MGO	MGO to HFO	HFO to MGO
load (%)	90	75	47	24	23	12	30	24
load (kW)	61,944	51,703	31,902	16,707	15,481	8,275	20,559	16,447
engine speed (rpm)	97	91	78	61	59	49	67	58
SFOC (g kW^{-1} h^{-1})	191	188	200	205	209	232	201	205

2-μm pore Teflo filters (Pall Gelman, Ann Arbor, MI). Loaded Teflo filters were weighed using a Mettler Toledo UMX2 microbalance following the guidelines within the Code of Federal Regulations (CFR).[20] Before and after the collection, the filters were conditioned for 24 h in an environmentally controlled room (RH = 40%, T = 25 °C) and weighed daily until two consecutive weight measurements were within 3 μg.[17] Teflo filters were subsequently extracted with HPLC-grade water and isopropyl alcohol and analyzed for sulfate ions using a Dionex DX-120 ion chromatograph. Sulfate on the Teflo filter PM was assumed to be in hydrated form ($H_2SO_4 \cdot 6H_2O$) as predicted using the aerosol thermodynamic model ISORROPIA.[32−34] Therefore, a factor of 2.15 was applied to the mass of sulfate ions to determine its total contribution to the PM mass. Parallel 2500 QAT-UP Tissuquartz Pall (Ann Arbor, MI) 47-mm filters (preconditioned at 600 °C for a minimum of 5 h) were used to collect $PM_{2.5}$ for subsequent elemental and organic carbon (EC/OC) analysis following the NIOSH[21] method using a Sunset Laboratory (Forest Grove, OR) thermal/optical carbon aerosol analyzer.

The real-time PM mass concentration in the dilution tunnel was monitored with a TSI DustTrak model 8520 taken directly from the tunnel and without a 2.5-μm cyclone separator. This measurement provided assurance that the PM concentration was steady while the mass was collected on the filters. A secondary dilution tunnel was installed to obtain particle NSD using a TSI scanning mobility particle sizer (SMPS) model-3080 with 3081 classifier and TSI 3772 condensation particle counter (CPC).

RESULTS AND DISCUSSION

Triplicate measurements were made consecutively across all loads. EFs are reported as grams per kilowatt-hour (gkW^{-1} h^{-1}) based on the concentration of measured species, recorded engine load, and calculated exhaust flow rate. The exhaust flow rate for the vessel was calculated assuming complete conversion of fuel carbon to carbon dioxide (carbon balance method).

Modal Emission Factors. Modal EFs are determined at steady-state conditions and are important for OGVs and locomotives as those engines normally operate for long periods of time at steady-state conditions or modes. Thus, modal EFs are essential for estimating inventories in a particular area. Modal EFs for CO, CO_2, NO_x, and SO_2 are summarized in Table 3. The modal value for NO_x at 75% engine load is just below the Tier 1 limit (17.0 gkW^{-1} h^{-1}) and close to the Tier 2 limit (14.4 gkW^{-1} h^{-1}) at 47% load. The modal EF_{CO2} also reflects fuel efficiency at different operating modes. EF_{CO2} is lowest at 75% load (590 gkW^{-1} h^{-1}) where OGVs spend a significant amount of time during transit.

The modal EFs for $PM_{2.5}$ mass, EC/OC, hydrated sulfate ($H_2SO_4 \cdot 6H_2O$), and ash are summarized in Table 4. The $PM_{2.5}$ mass was composed of 69−82% hydrated sulfate, 10−19% OC, <5% EC, and ash. EC and OC emissions decreased with increasing load (reflecting the engine efficiency tuning at 75% load) while sulfate emissions increased with increasing load. Fuel sulfur conversion to sulfate increased from 2.4% to 4.2% as the engine load increased from 24% to 90%, consistent with previous studies.[18,23]

Table 3. Modal Emission Factors (gkW^{-1} h^{-1}) of Different Gases for Main Engine

load (%)	fuel	CO_2	NO_x	CO	SO_2
12	MGO	749 ± 11	26.4 ± 1.5	0.39 ± 0.002	0.76
23	MGO	672 ± 1	16.8 ± 0.1	1.9 ± 0.09	0.68
24	HFO	644 ± 29	14.9 ± 0.2	1.7 ± 0.71	10.1
47	HFO	626 ± 15	14.4 ± 0.1	1.2 ± 0.07	9.86
75	HFO	590 ± 2	16.9 ± 0.2	0.32 ± 0.02	9.29
90	HFO	600 ± 5	15.2 ± 0.1	0.36 ± 0.004	9.44
30	MGO to HFO	654 ± 30[a]	15.8 ± 0.5[a]	2.09 ± 0.3[a]	n/a
24	HFO to MGO	651 ± 20[a]	16.1 ± 0.3[a]	1.44 ± 0.4[a]	n/a

[a]Average EFs during the fuel switch.

The main propulsion engine was operated at 24% (HFO) and 23% (MGO) allowing for a comparison of the $PM_{2.5}$ mass emissions. Results in Table 4 show the EF for $PM_{2.5}$ mass was reduced by ∼70% by switching to MGO with lower sulfur content. This reduction is significant and shows the impact of $PM_{2.5}$ emissions on communities near coastlines can be substantially mitigated by switching to a cleaner fuel, MGO.[24,25]

Modal Data for Particulate Diameters. The SMPS provided near continuous determination of the particle NSD for different operating modes and different fuels (Figure 1a). The exhaust particle NSDs for MGO are monodisperse with a mobility mode diameter at ∼30 nm when operating at <25% load. A slight increase in the mobility diameter is observed as load increases. In contrast, the particle NSD data for the HFO show the aerosol is distinctly bimodal with first mode at ∼35 nm and second mode between 70 and 95 nm. The shift to a larger diameter is consistent with the higher PM mass levels measured on the filters when the engine operated on HFO. Assuming constant particle density, particle volume distributions (Figure 1b) indicate a decrease in particulate mass with decreasing engine load.

Overall Emission Factors. The overall measured EFs were calculated (eq 2) for an engine operating on HFO with the weighting factors established in the ISO 8178-4 E3 protocols (Table 5). The equation for calculating the overall EF is

$$\mathrm{WEF} = \frac{\sum \mathrm{MEF} \times \mathrm{MWF}}{\sum \mathrm{Load} \times \mathrm{MWF}} \quad (2)$$

where

WEF: weighted emission factor ($gkW^{-1}h^{-1}$)
MEF: modal emission factor (gh^{-1})
MWF: ISO weighting factor for the mode
Load: engine load for the mode (kW)

Results show the overall EF_{CO2} was 600 ± 2 gkW^{-1} h^{-1} and similar to values reported in other studies.[17,22] As expected, the EF_{CO} of 0.5 ± 0.04 gkW^{-1} h^{-1} was much lower than that

dx.doi.org/10.1021/es2043646 | Environ. Sci. Technol. 2012, 46, 5049−5056

Table 4. Modal Emission Factors ($gkW^{-1}\ h^{-1}$) of $PM_{2.5}$ and Speciated $PM_{2.5}$ for Main Engine

load (%)	fuel	$PM_{2.5}$	EC	OC	$H_2SO_4 \cdot 6H_2O$	ash
12	MGO	0.28 ± 0.04	0.0023 ± 0.002	0.17 ± 0.003	0.05 ± 0.01	0.02
23	MGO	0.34 ± 0.07	0.0034 ± 0.0003	0.17 ± 0.01	0.08 ± 0.02	0.02
24	HFO	1.19 ± 0.05	0.0087 ± 0.002	0.22 ± 0.006	0.79 ± 0.05	0.14
47	HFO	1.22 ± 0.05	0.0057 ± 0.0004	0.19 ± 0.002	0.90 ± 0.06	0.14
75	HFO	1.44 ± 0.04	0.0043 ± 0.001	0.17 ± 0.001	1.13 ± 0.11	0.13
90	HFO	1.54 ± 0.04	0.0039 ± 0.0002	0.16 ± 0.003	1.28 ± 0.02	0.13

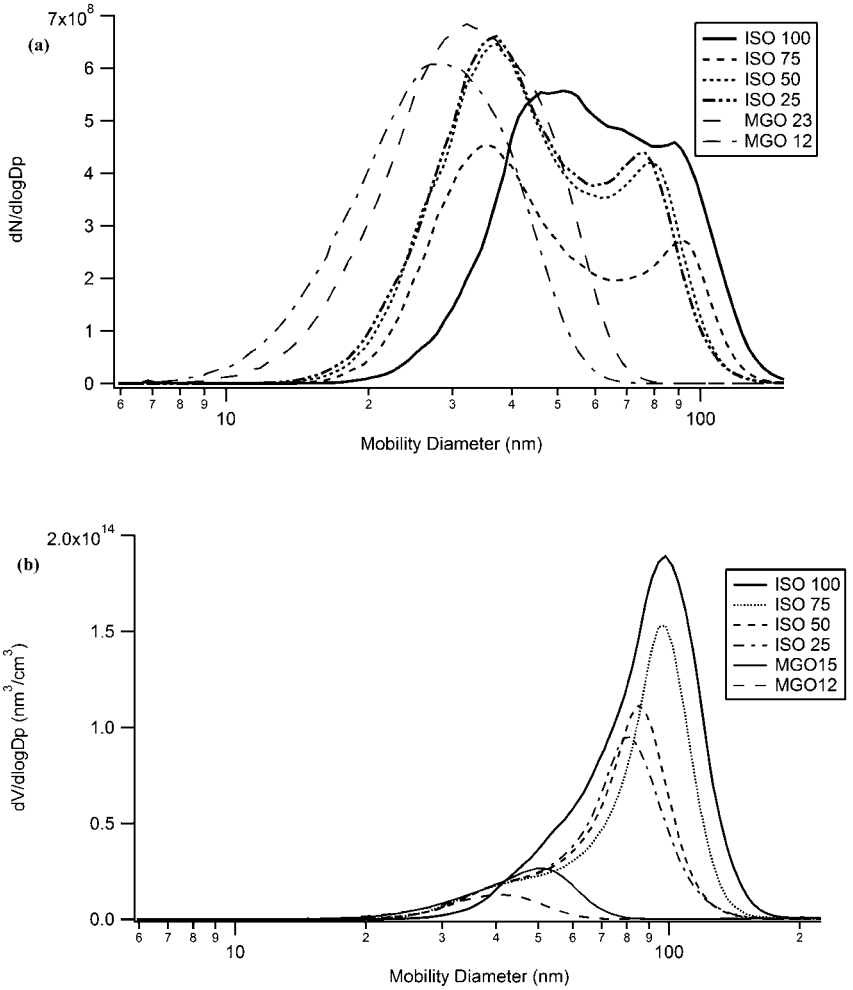

Figure 1. Particle number (a) and volume concentrations (b) for all operating modes.

Table 5. Comparison of Measured Overall Emission Factors with Others

	NO_x	$PM_{2.5}$	SO_2[a]	CO_2
measured	16.1 ± 0.1	1.42 ± 0.04	9.44	600 ± 2
Agrawal[17]	18.21	1.63	8.39	644
Agrawal[23]	19.77 ± 0.28	2.40 ± 0.05	11.53	617
Llyods service data[26]	18.7	1.23	-	-
U.S. EPA 2009[27]	18.1	1.31	10.29	620
CARB 2008[22]	18.1	1.46	10.50	620

[a] SO_2 values reported are calculated from sulfur in the fuel.

measured for CO_2 as most of the carbon (99.9%+) in the fuel was converted to CO_2. Results in Table 5 show the overall EF_{NOx} was about 14% lower than the Lloyd's values and 5% lower than the Tier 1 certification value. EF for $PM_{2.5}$ mass is strongly dependent on the sulfur content of the fuel and therefore hard to compare with previous work. Comparative values for EC[23] indicate the overall EF is lower, suggesting an improved combustion process.

Transient Data. Although OGVs generally operate at a fixed load, there are times when the engine operates in a transient mode. For example, transient modes can occur when maneuvering and entering or leaving the harbor. Another transient period is during the fuel switch from HFO to MGO or from MGO to HFO. Transient data are quite scarce, as are the opportunities for taking such measurements. During this research we continuously measured the gaseous and PM concentrations and particle NSD transitions during the fuel switching operations. As the vessel left the harbor, it operated on MGO and then beyond 24 nmi the vessel switched from MGO to HFO. Fuel switching takes time as the crew carefully follows a detailed checklist for fuel switching that was prepared in consultation with the engine manufacturer. According to engine manufacturers, rapidly changing fuel and/or temperature will

dx.doi.org/10.1021/es2043646 | Environ. Sci. Technol. 2012, 46, 5049–5056

move viscosity outside the specified range and harm the fuel delivery system, including pumps and injectors. Therefore, switchover must be carried out slowly in order to avoid scuffing of fuel valves, fuel pump plungers, and suction valves.[30]

Figure 2a shows the continuous emissions data as the vessel switched fuels. During the switch, vessel load was ~30%, except for two times at ~9:08 and ~9:43 a.m. when small perturbations occurred. As a consequence of the constant load, the gas-phase emissions for NO_x, CO, and CO_2 did not change significantly; however, the real-time EF_{SO2} and particle NSD took about ~55 min to reach steady-state again. Figure 2b shows the transient behavior of the particle mode diameter and particle number concentrations during the fuel switch. The results show a new particle mode occurred within a few minutes of the fuel switch from 35 to 75 nm; leading to the formation of a bimodal particle NSD within 1 hour. The transient particle NSD data are consistent with observations of particle NSD for steady-state mode testing using HFO.

When nearing the coastline the vessel switched from HFO to MGO at about 24% load. With the load constant, the concentrations of NO_x, CO, and CO_2 were basically steady; however, the EF_{SO2} and particle NSD decreased over the ~84 min needed to achieve steady state (Figure 2c). Transient particle NSD data (Figure 2d) show the initial bimodal distribution returns to a single mode, as expected for MGO. Although total particle number decreased gradually along with SO_2, high concentrations of smaller particles were observed throughout the fuel switch which is an indication of the presence of HFO in the fuel feed even 84 min after the fuel switch commenced.

Except for SO_2, the averages of transient EFs (Table 3) for fuel switching are calculated. SO_2 concentrations exhibit nonlinear change due to continuous changes in the fuel sulfur content. EF_{SO2} (gkW^{-1} h^{-1}) changed from 0.7 to 11 during fuel switching from MGO to HFO and 10.1 to 0.7 from HFO to MGO. In both switches, rapid change in EFs was observed (Figure 2a, c) during the early stage of mixing fuels which tends to slow down in the rest of the fuel switch. Because of its nonlinear behavior, EF_{SO2} cannot be averaged out for the entire fuel switch and requires continuous monitoring of SO_2 concentration or an equation that can predict change in sulfur content of the mixing fuel (see Figure S1).

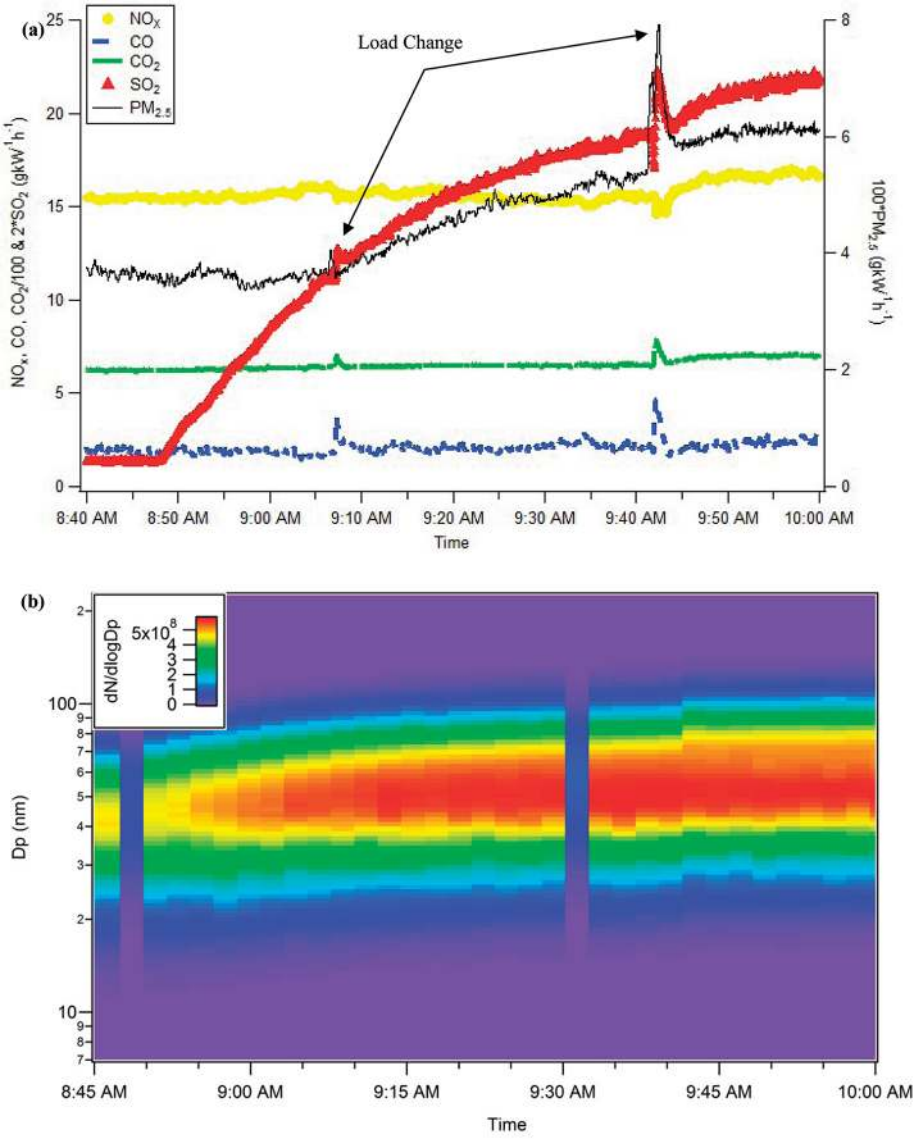

Figure 2. continued

dx.doi.org/10.1021/es2043646 | *Environ. Sci. Technol.* 2012, 46, 5049–5056

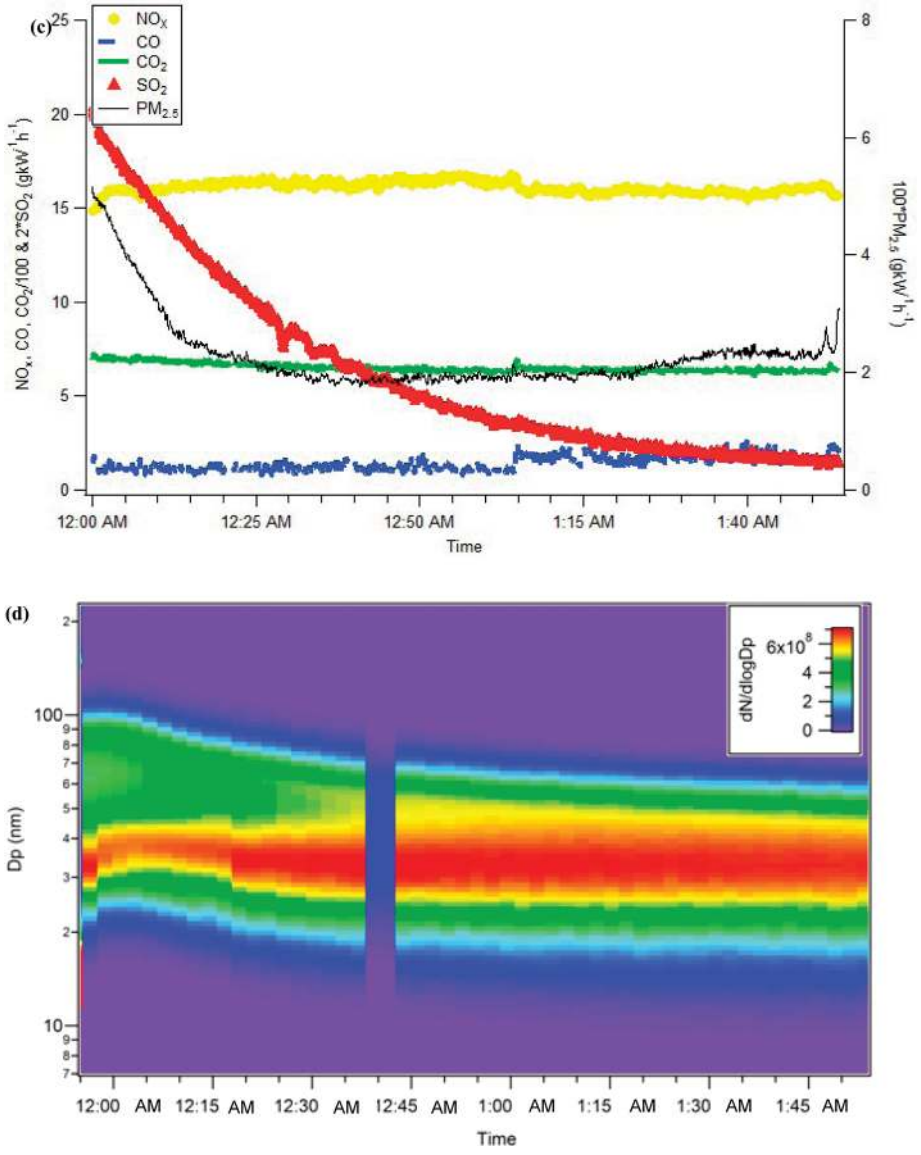

Figure 2. Real-time (a) gaseous EFs ($gkW^{-1}\ h^{-1}$) and (b) particle number concentration measurement when fuel was switched from MGO to HFO at 30% engine load. Change in load was observed at 9:08 and 9:43 a.m. Note: CPC 3772 data were not available around 8:50 a.m. and 9:30 a.m. Real-time (c) gaseous EFs ($gkW^{-1}\ h^{-1}$) and (d) particle number concentration measurement when fuel was switched from HFO to MGO at 24% engine load. Note: CPC 3772 data were not available around 12:40 a.m.

The times measured for a fuel change during this research were substantial and surprisingly long. These results can be compared with earlier research by our group where the times were also measured (Table 6). Taken in total it is evident that the long times measured in this research are representative of the time required for a fuel switch to be completed when following the checklist and procedure developed by the engine manufacturer.

Table 6. Fuel Switching Time (t_{95}) for Different Vessels

	vessel 1[a]	vessel 1[b]	vessel 2	vessel 3[c]
$t_{\text{MGO to HFO}}$ (min)	60	70	80	55
$t_{\text{HFO to MGO}}$ (min)	-	90	-	84

[a]Trip I on vessel 1. [b]Trip II on vessel 1. [c]Current study.

Nonlinear Mixing Equation. Because the time required for the fuel switch was about an hour, rather than minutes, a simple kinetic equation was independently developed with the goal of identifying the primary parameters that control the length of time required for 95% switchover of the fuel, t_{95}. Developing an equation required a schematic of the fuel flow system model for a marine engine (Figure 3) and some assumptions, including (1) ideal mixing in the day tank, (2) the rate of fuel to the engine, $E \gg R$, the fuel rate in the return line, (3) perturbations in load due to variations in the sea state are insignificant, and (4) t_{95} is not affected by changes in fuel viscosity. With these assumptions, t_{95} can be parameterized as a function of net fuel consumption rate, f (L min^{-1}), and volume of the fuel in the day tank, V_{DT} (L), eq 3.

$$t_{95} = \frac{V_{DT}}{f} \ln 20 \tag{3}$$

The output of this equation is compared with the observed time needed for fuel switch in this study. Comparisons are presented here as Case I (MGO to HFO, f = 77 L min^{-1}) and Case II (HFO to MGO, f = 65 L min^{-1}). V_{DT} reported for this

dx.doi.org/10.1021/es2043646 | Environ. Sci. Technol. 2012, 46, 5049–5056

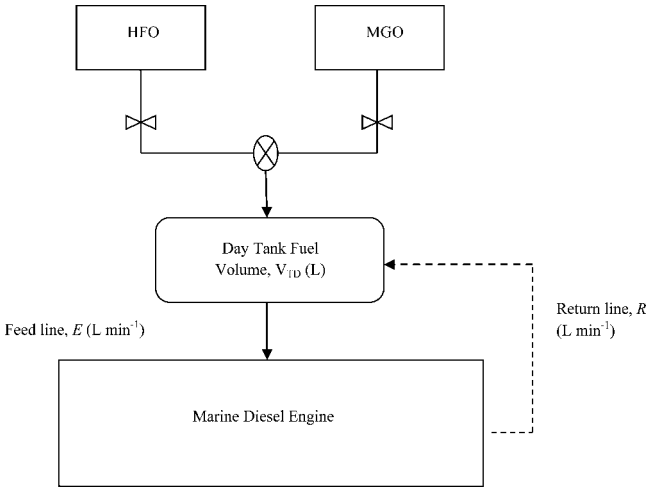

Figure 3. Fuel flow system for marine diesel engine.

study was 1500 L in both cases. The t_{95} calculated by the equation is equal to 59 and 69 min, for Case I and Case II, respectively. With 95% change in fuel for Case I, the expected SO_2 concentration would be 435 ppm after 65 min of fuel switching and agrees with calculated values from eq 3. Similarly, in Case II, expected SO_2 concentration is 50 ppm after 84 min of fuel switching. The comparison of measured and calculated SO_2 concentrations with time is shown in Figure S1. Additional measurements are required to account for uncertainties associated with eq 3. A detailed derivation for the equation is provided in Supporting Information.

Note the eq 3 predicts the longer time to switch for Case II since the load and corresponding fuel rate were lower. The key parameters driving the length of time for the fuel switch are the volume of fuel in the day tank and the rate of fuel consumption. Equation 3 predicts that the time required for fuel switching for an OGV can be reduced by either decreasing the volume of fuel in the day tank or by increasing the rate of fuel consumption or both.

Implications. The results of the research measured the significant benefits for two mitigation strategies: cleaner engines and cleaner fuels. The actual in-use EF_{NOx} was 5% and 14% lower than the Tier 1 certification value and the Lloyds service data commonly used in the development of emission inventories, respectively. The overall in-use EF_{EC} and EF_{OC} were 33% and 20% lower than the comparative post-Panamax container vessel studied by Agrawal et al.,[23] reflecting the benefits of newest engine technologies. This research also verified an equation to calculate the length of time for a fuel switch. Given that vessels do not have monitoring equipment to calculate the length of time to switch fuels, vessels may switch at the distance specified in the regulation. While this approach is practical, regulated boundaries close to the ports for burning cleaner fuels will not provide the intended protection for people's health. For example, a large container vessel operating at a speed of 15 knots and requiring 85 min for fuel switching will have traveled 21 nmi within the 24 nmi regulated zone with elevated SO_2 and $PM_{2.5}$ emissions. Even at lower speeds, there will be a significant increase in OGV emissions on the port communities. From a global perspective, the increase in emissions when entering the harbor will be offset by the decrease in emissions on leaving the harbor. However, the interest is in the health of people in local port communities. Therefore, it is important to set the regulatory boundary far enough from the port so that the time required to switch to cleaner fuel becomes a trivial issue.

■ ASSOCIATED CONTENT

Supporting Information

Additional selected specifications of vessel and engine and detailed derivation of the equation to predict switchover time. This material is available free of charge via the Internet at http://pubs.acs.org.

■ AUTHOR INFORMATION

Corresponding Author

*E-mail: dcocker@engr.ucr.edu.

Notes

The authors declare no competing financial interest.

■ ACKNOWLEDGMENTS

This study would have not been possible without the funding from the United States Environmental Protection Agency and the California Air Resources Board, the analytical support from Ms. Kathy Cocker, the shipping company that provided the opportunity, and the helping hands of the crew on the vessel. We also thank Dr. Varalakshmi Jayaram, Mr. Charles Bufalino for test preparation, and Ms. Poornima Dixit, Mr. David Torres, and Mr. Charles Wardle for their support in analyses of the sample media.

■ REFERENCES

(1) Capaldo, K.; et al. Effects of ship emissions on sulphur cycling and radiative climate forcing over the ocean. *Nature* **1999**, *400* (6746), 743−746.

(2) Duce, R. A.; et al. Impacts of atmospheric anthropogenic nitrogen on the open ocean. *Science* **2008**, *320* (5878), 893−897.

(3) Lauer, A.; et al. Assessment of Near-Future Policy Instruments for Oceangoing Shipping: Impact on Atmospheric Aerosol Burdens and the Earth's Radiation Budget. *Environ. Sci. Technol.* **2009**, *43* (15), 5592−5598.

(4) Agrawal, H.; et al. Primary Particulate Matter from Ocean-Going Engines in the Southern California Air Basin. *Environ. Sci. Technol.* **2009**, *43* (14), 5398−5402.

(5) Song, S. K.; et al. Influence of ship emissions on ozone concentrations around coastal areas during summer season. *Atmos. Environ.* **2010**, *44* (5), 713−723.

(6) Corbett, J. J. Mortality from Ship Emissions: A Global Assessment. *Environ. Sci. Technol.* **2007**, *41* (24), 8512−8518.

(7) Winebrake, J. J.; et al. Mitigating the Health Impacts of Pollution from Oceangoing Shipping: An Assessment of Low-Sulfur Fuel Mandates. *Environ. Sci. Technol.* **2009**, *43* (13), 4776−4782.

(8) Title 13 Section 2299.3. California Code of Regulations.

(9) Kasper, A.; et al. Particulate emissions from a low-speed marine diesel engine. *Aerosol Sci. Technol.* **2007**, *41* (1), 24−32.

(10) Petzold, A.; et al. Physical Properties, Chemical Composition, and Cloud Forming Potential of Particulate Emissions from a Marine Diesel Engine at Various Load Conditions. *Environ. Sci. Technol.* **2010**, *44* (10), 3800−3805.

(11) Moldanova, J.; et al. Characterisation of particulate matter and gaseous emissions from a large ship diesel engine. *Atmos. Environ.* **2009**, *43* (16), 2632−2641.

(12) Fridell, E.; Steen, E.; Peterson, K. Primary particles in ship emissions. *Atmos. Environ.* **2008**, *42* (6), 1160−1168.

(13) Lyyranen, J.; Jokiniemi, J.; Kauppinen, E. The effect of Mg-based additive on aerosol characteristics in medium-speed diesel engines operating with residual fuel oils. *J. Aerosol Sci.* **2002**, *33* (7), 967−981.

(14) Lyyranen, J.; et al. Aerosol characterisation in medium-speed diesel engines operating with heavy fuel oils. *J. Aerosol Sci.* **1999**, *30* (6), 771−784.

(15) Murphy, S. M.; et al. Comprehensive Simultaneous Shipboard and Airborne Characterization of Exhaust from a Modern Container Ship at Sea. *Environ. Sci. Technol.* **2009**, *43* (13), 4626−4640.

(16) ISO. *ISO 8178-2, Reciprocating Internal Combustion Engines: Exhaust Emission Measurement. Part-2: Measurement of Gaseous*

Particulate Exhaust Emissions at Site; International Organization of Standardization, 1996.
(17) Agrawal, H.; et al. In-use gaseous and particulate matter emissions from a modern ocean going container vessel. *Atmos. Environ.* **2008**, *42* (21), 5504−5510.
(18) Agrawal, H.; et al. Emission measurements from a crude oil tanker at sea. *Environ. Sci. Technol.* **2008**, *42* (19), 7098−7103.
(19) ISO. 8178-1, 1st edition; International Organization for Standardization, 1996.
(20) Protection of the Environment. Title 40. Sections 86 and 89. U.S. Code of Federal Regulations.
(21) NIOSH. *NIOSH Manual of Analytical Methods*; National Institute of Occupational Safety and Health: Cincinnati, OH, 1996.
(22) CARB, California Air Resources Board. *Emissions Estimation Methodology for Ocean-going Vessels*; 2008.
(23) Agrawal, H., et al. Emissions from main propulsion engine on container ship at sea. *J. Geophys. Res.-Atmos.*, 2010 *115*.
(24) IMO 2000. *Study of Greenhouse Gas Emissions from Ships-Final Report*; 2000.
(25) Corbett, J. J. Global Nitrogen and Sulfur Emissions Inventories for Oceangoing Ships. *J. Geophys. Res.-Atmos.* **1999**, *104*, 3457−3470.
(26) Entec UK Limited. *Quantification of Emissions from Ships associated with Ship Movements between Ports in the European Community*; 2002.
(27) U.S. EPA. *Current Methodologies in Preparing Mobile Source Port-Related Emission Inventories*, 2009.
(28) Baranescu, R. A., *Influence of Fuel Sulfur on Diesel Particulate Emissions*; SAE Technical Paper Series 881174; 1988.
(29) Wall, J. C.; Shimpi, S. A.; Yu, M. L. *Fuel Sulfur Reduction for Control of Diesel Particulate Emissions*; SAE, 1988.
(30) *Technical considerations of fuel switching practices*. API Technical Issues Workshop; June, 3, 2009.
(31) Lloyd's Register. *Lloyd's Register Engineering Services*; 1990a, 1990b, 1993a, 1993b, 1995.
(32) Nenes, A.; Pilinis, C.; Pandis, S. N. ISORROPIA: A New Thermodynamic Model for Multiphase Multicomponent Inorganic Aerosols. *Aquat. Geochem.* **1998**, *4*, 123−152.
(33) Fountoukis, C.; Nenes, A. ISORROPIA II: A Computationally Efficient Aerosol Thermodynamic Equilibrium Model for K^+ - Ca^{2+} - Mg^{2+} - NH_4^+ - SO_4^{2-} - NO_3^- - - Cl^- - H_2O Aerosols. *Atmos. Chem. Phys.* **2007**, *7*, 4639−4659.
(34) ISORROPIA. http://nenes.eas.gatech.edu/ISORROPIA.
(35) MAN Diesel Low Speed. Marine Diesel Engines. Marine Diesel Engines Improvements on the Efficiency. http://www.dtu.dk/upload/institutter/kt/nyheder/cccs_pres/man_diesel-soeren_h_jensen.pdf.